Multibody System Dynamics **10:** 363–391, 2003.

An Efficient Multibody Dynamics Model for Internal Combustion Engine Systems

ZHENG-DONG MA and NOEL C. PERKINS
Department of Mechanical Engineering, The University of Michigan, Ann Arbor, MI 48109, U.S.A.; E-mail: {mazd,ncp}@umich.edu

(Received: 4 March 2002; accepted in revised form: 2 December 2002)

Abstract. The equations of motion for the major components in an internal combustion engine are developed herein using a recursive formulation. These components include the (rigid) engine block, pistons, connecting rods, (flexible) crankshaft, balance shafts, main bearings, and engine mounts. Relative coordinates are employed that automatically satisfy all constraints and therefore lead to the minimum set of ordinary differential equations of motion. The derivation of the equations of motion is automated through the use of computer algebra as the precursor to automatically generating the computational (C or Fortran) subroutines for numerical integration. The entire automated procedure forms the basis for an *engine modeling template* that may be used to support the *up-front design* of engines for noise and vibration targets. This procedure is demonstrated on an example engine under free (idealized) and firing conditions and the predicted engine responses are compared with results from an ADAMS model. Results obtained by using different bearing models, including linear, nonlinear, and hydrodynamic bearing models, are discussed in detail.

Key words: engine modeling, recursive algorithm, symbolic programming, journal bearing, flexible MBD.

1. Introduction

Finite element techniques are frequently employed in evaluating the dynamic response of well-defined engine designs; see, for example, [1–9]. The finite element models require detailed geometric and material data of the engine components, as well loading data defined by engine combustion forces (and possible coupling with the remainder of the powertrain). At the start of an engine design, this information is simply unavailable. Nevertheless, the need exists at the start of the engine design cycle to estimate the dynamics of an engine and to a degree needed to verify performance targets. To this end, simplified engine models have been proposed for estimating some performance measures. For instance, a rigid body engine block model may be used for designing engine mounting systems (e.g., 10–13]). These models, however all ignore the dynamic coupling with the crankshaft. More recent models [14–16] include one-way coupling of the crankshaft motion on the engine block, but then ignore the crankshaft and bearing flexibility that is needed to estimate bearing reaction loads. By contrast, models that incorporate

crankshaft and bearing flexibility [17–19], typically ignore the engine mounting system, and consider the motion of the pistons and connecting rods as prescribed functions. Thus, the coupling effects of the crankshaft flexibility with the engine mounting system and with the piston-rod motion are ignored. Two recent studies [20, 21] stress the importance of developing complete and fully coupled engine models.

Fully coupled engine models can be constructed through the use of commercial multibody dynamics codes, such as ADAMS and DADS; see, for example [22–25]. These commercial codes provide a modeling platform for very general mechanical systems and the time and effort required to learn how to use these codes may preclude their use for the non-expert who also desire quick estimates for differing engine designs at the very start of the design cycle.

In this paper, an alternative and specialized modeling platform is developed that functions as a 'template' for engine design. Relative to commercial codes, this engine design template leads directly to the minimum number of equations of motion describing the dynamic response of the engine by *a priori* satisfaction of kinematic constraints. This is achieved by employing relative coordinates in lieu of the absolute coordinates adopted in commercial multibody dynamics codes. This engine modeling tool requires only minimum information for the input data. As a further benefit, the engine models herein, are cast purely as a (minimum) set of ordinary differential equations of motion in lieu of the differential-algebraic equations that result from using commercial multibody dynamics codes. These differences lead to engine models that may be built with minimum inputs and also integrated with greater efficiency.

The objective of this paper is to review the basic formulation that forms the core of the engine modeling template (*EngTmp*) for the up-front design of engines for noise and vibration targets. This paper begins by describing engine kinematics, the relative coordinates, and the independent coordinates used for the recursive formulation. Next, D'Alembert's principle is employed to automatically generate the equations of motion using symbolic-computation. Computational code is then developed from this result for use in *EngTmp*. This procedure significantly reduces the cost involved in developing the recursive model and also reduces the possibility of coding errors. Three critical modeling issues are addressed in this formulation; namely the engine mounts, the journal bearings, and the flexible crankshaft. The *EngTmp* is then used to evaluate the response of an example engine under free (idealized) and firing conditions and the predicted engine responses are compared with results from an ADAMS model. Results obtained by using different bearing models, including linear, nonlinear, and hydrodynamic bearing models, are discussed in detail. We begin by describing the kinematical quantities.

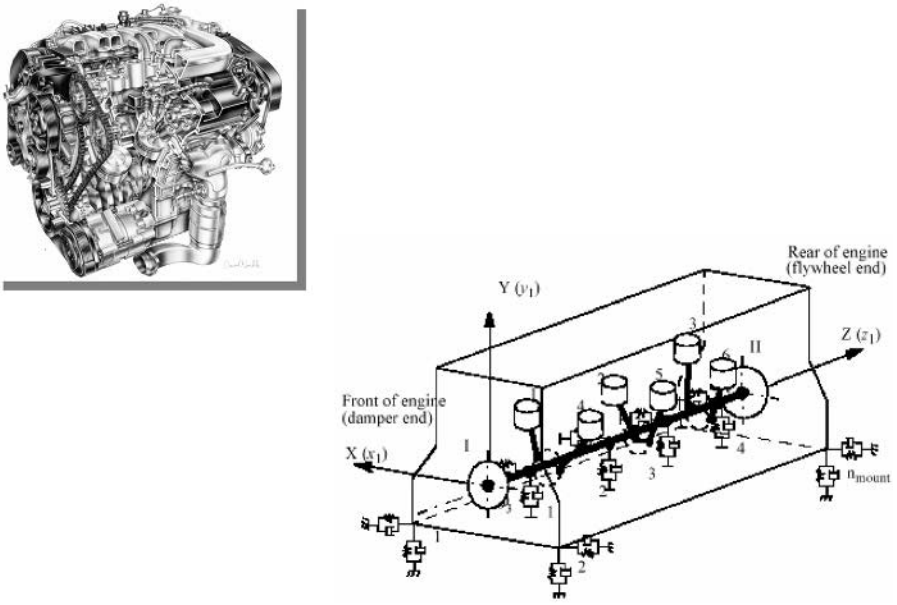

Figure 1. An example V-6 engine model.

2. Engine Kinematics

The kinematical quantities to describe the engine dynamics are key issue to the modeling approach developed in this paper. We employ relative coordinates as generalized coordinates. Figure 1 shows the structure of an example engine (Ford 2.5L-V6). The critical components to be modeled include the engine block with six cylinders ($n_{\text{cylinder}} = 6$), a crankshaft supporting six pairs of pistons and connecting rods, a balance shaft, four main journal bearings ($n_{\text{journal}} = 4$), and four engine mounts ($n_{\text{mount}} = 4$). A traditional approach in modeling a multi-body system such as this engine is to assign six degrees-of-freedom (dof) to each individual rigid body and then to satisfy the kinematic constraint equations and the equations of motion simultaneously during integration. In this example, composed of 15 individual bodies, this approach produces a model with 90 degrees of freedom subject to 78 constraints. The remaining 12 dof are required to uniquely describe the position and orientation of the engine block (6 dof), and the position and orientation of the rigid crankshaft relative to the engine block (6 dof). (Note that the crankshaft is presently considered rigid for the purpose of this discussion.) The use of the constraint equations in this traditional formulation results in a set of differential-algebraic equations that is generally more difficult to integrate than ordinary differential equations alone. It is also possible to formulate this engine model in terms of just 12 ordinary differential equations provided one satisfies the constraints *a priori*. The key to doing so is to employ relative coordinates as described in the following section.

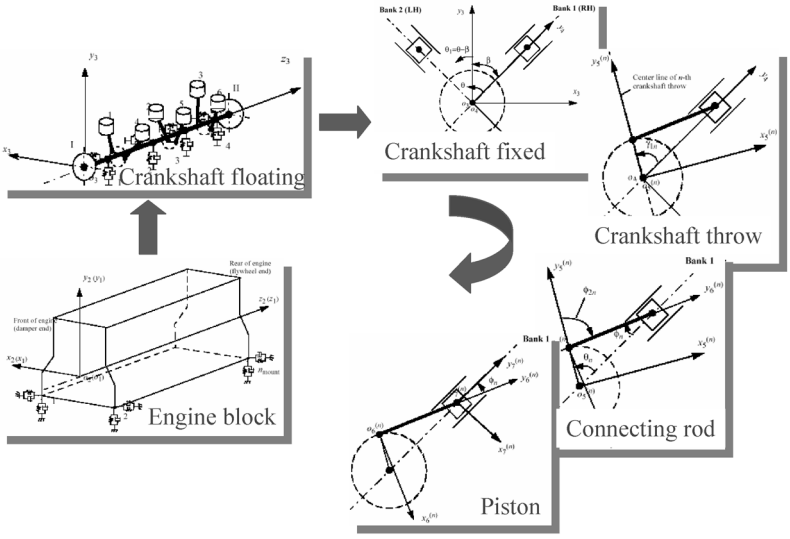

Figure 2. Relative coordinate systems.

2.1. RELATIVE COORDINATE SYSTEMS AND GENERALIZED COORDINATES

Seven coordinate systems, $o_i - x_i y_i z_i$ ($i = 1, 2, \ldots, 7$), are defined in the Appendix for use in the engine model as illustrated in Figure 2. Let of $o_i - x_1 y_1 z_1$ denote the vehicle coordinate system, $o_2 - x_2 y_2 z_2$ the engine block coordinate system, $o_3 - x_3 y_3 z_3$ the crankshaft floating coordinate system, $o_4 - x_4 y_4 z_4$ the crankshaft fixed coordinate system, $o_5 - x_5 y_5 z_5$ the crankshaft throw coordinate system, $o_6 - x_6 y_6 z_6$ the connecting-rod coordinate system, and $o_7 - x_7 y_7 z_7$ the piston coordinate system.

The components of a position vector in a coordinate system $o_i - x_i y_i z_i$ defined by

$$\mathbf{r}_i = \begin{Bmatrix} x_i \\ y_i \\ z_i \end{Bmatrix} \tag{1}$$

can be transformed into components in the coordinate system $o_{i-1} - x_{i-1} y_{i-1} z_{i-1}$ through

$$\mathbf{r}_{i-1} = \mathbf{d}_{i-1} + \mathbf{A}_{i-1,i} \mathbf{r}_i, \tag{2}$$

where $\mathbf{d}_{i-1}$ denotes the position vector of the origin of of $o_i - x_i y_i z_i$ relative to $o_{i-1} - x_{i-1} y_{i-1} z_{i-1}$, and $\mathbf{A}_{i-1,i}$ is the rotation matrix of $o_i - x_i y_i z_i$ with respect to $o_{i-1} - x_{i-1} y_{i-1} z_{i-1}$. Explicit expressions for $\mathbf{d}_{i-1}$ and $\mathbf{A}_{i-1,i}$ (where $i = 2, 3, \ldots, 7$) are provided in the Appendix.

Note that this formulation allows crankshaft flexibility to be captured. Here, the crankshaft is considered as a linear elastic body with small displacement at the

crankshaft-fixed coordinate system ($o_4 - x_4 y_4 z_4$). In particular, the displacement in the x_4–y_4 plane, which is perpendicular to the axis of the crankshaft, is considered to have appreciable influence on the motion of the pistons and connecting rods. The effect of longitudinal deformation of the crankshaft along the crankshaft axis has negligible influence on the motion of pistons and connecting rods, and therefore is ignored in this model.

Crankshaft deformations are described using a modal representation. Let ($\mathbf{\Phi} = [\phi_1, \phi_2, \ldots, \phi_{n_{\text{nodes}}}]$ represent a set of the selected crankshaft vibration mode shapes (describing bending and torsional modes of the crankshaft) and $\mathbf{p} = \{p_1, p_2, \ldots p_{n_{\text{modes}}}\}^T$ a set of corresponding modal coordinates, where p_i's are independent each other, and n_{modes} denotes the number of modes selected. Then the position of a point on the crankshaft at the crankshaft coordinate system ($o_4 - x_4 y_4 z_4$) can be described by the vector

$$\mathbf{r}_4 = \mathbf{r}_4^{(\text{rigid})} + \sum_{i=1}^{n_{\text{nodes}}} \phi_i p_i, \tag{3}$$

where $\mathbf{r}_4^{(\text{rigid})}$ denotes the position vector of the point with no crankshaft vibration (measured at the crankshaft fixed coordinate system).

Let γ_n denote the torsional deformation (angle) of the crankshaft at the nth crankshaft throw, which is the deformation angle occurred between axes $y_5^{(n)}$ and y_4 in Figure 14 due to the crankshaft torsional deformation. Let ε_n denote the radial displacement of the center of the nth pin joint at the crankshaft, which is measured along axis $y_5^{(n)}$ direction shown in Figure 14. These quantities can be written as the functions of the modal coordinates using Equation (3), and then used in kinematic relationships of the relative coordinate systems as detailed in the Appendix.

A minimal set of the general coordinates for the engine model is then chosen as:

$$\mathbf{q} = \{q_i\} = \{u_b, v_b, w_b, \alpha_b, \beta_b, \gamma_b, u_c, v_c, w_c, \alpha_c, \beta_c, p_i, p_2, \ldots, p_{n_{\text{modes}}}, \theta\}^T, \tag{4}$$

where u_b, v_b, w_b denote the coordinates of the origin of the engine block frame with respect to the vehicle body, $\alpha_b, \beta_b, \gamma_b$ denote the Euler angles of the engine block with respect to the vehicle body, u_c, v_c, w_c denote the coordinates of the origin of the crankshaft frame (namely $o_3 - x_3 y_3 z_3$) with respect to the vehicle body, $\alpha_c, \beta_c, \gamma_c$ denote the Euler angles of the crankshaft axis with respect to the vehicle body, p_i ($i = 1, 2, \ldots, n_{\text{modes}}$) denote the modal coordinates for the selected n_{modes} number of crankshaft vibration modes, and θ denotes the crankshaft rotation angle from top dead center (TDC). Note that $\gamma_c \equiv \gamma_b$ as the relative rigid body rotation between the crankshaft and the block about the z axis is determined by the crankshaft angle θ. Also note that the Euler angles, $\alpha_b, \beta_b, \gamma_b, \alpha_c, \beta_c$, are assumed to be sufficiently small so that subsequent nonlinear terms in these angles can be ignored. The total number of generalized coordinates in the engine model is therefore

$$n_{\text{dof}} = 11 + n_{\text{modes}} \quad \text{or} \quad n_{\text{dof}} = 12 + n_{\text{modes}} \tag{5}$$

depending on whether the crankshaft angle θ is prescribed (as in a steady-state analysis) or treated as an independent degree of freedom (as in a transient analysis).

2.2. DISPLACEMENTS, VELOCITIES, AND ACCELERATIONS IN TERMS OF THE GENERALIZED COORDINATES

Equation (2) can be rewritten in a more compact form by using the 4×4 transform matrix,

$$\mathbf{R}_{i-1} = \mathbf{C}_{i-1,i}\mathbf{R}_i, \tag{6}$$

where

$$\mathbf{R}_i = \begin{Bmatrix} \mathbf{r}_i \\ 1 \end{Bmatrix} \quad \text{and} \quad \mathbf{C}_{i-1,i} = \begin{bmatrix} \mathbf{A}_{i-1,i} & \mathbf{d}_{i-1} \\ 0 & 1 \end{bmatrix}. \tag{7}$$

The inverse relation between vectors $\mathbf{r}_i$ and $\mathbf{R}_i$ therefore is

$$\mathbf{r}_i = \mathbf{D}\mathbf{R}_i \quad \text{where} \quad \mathbf{D} = \begin{bmatrix} 1 & 0 & 0 & 0 \\ 0 & 1 & 0 & 0 \\ 0 & 0 & 1 & 0 \end{bmatrix}. \tag{8}$$

Using Equations (6–8), the displacements in any local coordinate system $o_k - x_k y_k z_k$ can be transformed to the vehicle coordinate system $o_1 - x_1 y_1 z_1$ which serves as the global coordinate system. Thus,

$$\mathbf{r}_1 = \mathbf{D}\mathbf{C}_{1,k}\,\mathbf{R}_k, \tag{9}$$

where $k = 2, 3, \ldots,$ or 7, and

$$\mathbf{C}_{1,k} = \mathbf{C}_{1,2}\,\mathbf{C}_{2,3}\,\ldots\,\mathbf{C}_{k-1,k} = \mathbf{C}_{1,k-1}\,\mathbf{C}_{k-1,k}. \tag{10}$$

Using results from the Appendix, Equation (9) yields an explicit relationship between the displacements in a local coordinate system and the generalized coordinates introduced in Equation (4).

By differentiating Equation (9) we obtain

$$\dot{\mathbf{r}}_1 = \mathbf{D}(\mathbf{C}_{1,k}\,\dot{\mathbf{R}}_k + \dot{\mathbf{C}}_{1,k}\,\mathbf{R}_k), \tag{11}$$

where

$$\dot{\mathbf{C}}_{1,k} = \dot{\mathbf{C}}_{1,k-1}\,\mathbf{C}_{k-1,k} + \mathbf{C}_{1,k-1}\,\dot{\mathbf{C}}_{k-1,k}\,. \tag{12}$$

Therefore, the velocity components in any local coordinate system $o_k - x_k y_k z_k$ can be transformed to these in the global coordinate system by using Equation (11). Equation (11) defines an explicit relationship between the velocity components in a local coordinate system with the generalized coordinates $\mathbf{q}$ and their first derivatives $\dot{\mathbf{q}}$.

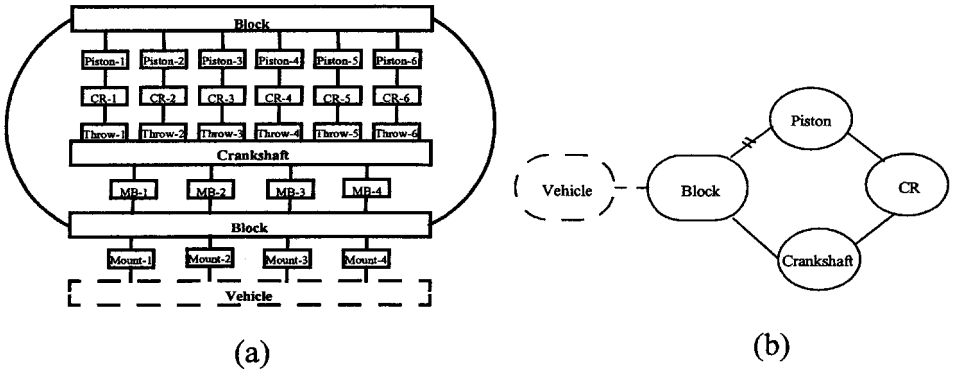

Figure 3. (a) Block diagram of typical V-6 engine structure, and (b) a closed kinematic loop of engine modeling chain.

By differentiating Equation (11) again, we obtain

$$\ddot{\mathbf{r}}_1 = \mathbf{D}(\mathbf{C}_{1,k}\,\ddot{\mathbf{R}}_k + 2\dot{\mathbf{C}}_{1,k}\,\dot{\mathbf{R}}_k + \ddot{\mathbf{C}}_{1,k}\,\mathbf{R}_k), \tag{13}$$

where

$$\ddot{\mathbf{C}}_{1,k} = \ddot{\mathbf{C}}_{1,k-1}\,\mathbf{C}_{k-1,k} + 2\dot{\mathbf{C}}_{1,k-1}\,\dot{\mathbf{C}}_{k-1,k} + \mathbf{C}_{1,k-1}\,\ddot{\mathbf{C}}_{k-1,k}\,. \tag{14}$$

Therefore, the acceleration components in any local coordinate system $o_k - x_k y_k z_k$ can be transformed to those in the global coordinate system by using Equation (13). Equation (13) defines an explicit relationship of the accelerations in a local coordinate system with $\mathbf{q}$, $\dot{\mathbf{q}}$, and $\ddot{\mathbf{q}}$.

2.3. VIRTUAL DISPLACEMENTS IN TERMS OF THE GENERALIZED COORDINATES

By taking the variation of Equation (9), the virtual displacements in any local coordinate system $o_k - x_k y_k z_k$ become

$$\delta\mathbf{r}_1 = \mathbf{D}(\mathbf{C}_{1,k}\,\delta\mathbf{R}_k + \delta\mathbf{R}_k + \delta\mathbf{C}_{1,k}\,\mathbf{R}_k), \tag{15}$$

where

$$\delta\mathbf{C}_{1,k} = \delta\mathbf{C}_{1,k-1}\,\mathbf{C}_{k-1,k} + \mathbf{C}_{1,k-1}\,\delta\mathbf{C}_{k-1,k}\,. \tag{16}$$

Equation (15) defines an explicit relationship of the virtual displacements in a local coordinate system with $\mathbf{q}$ and $\delta\mathbf{q}$.

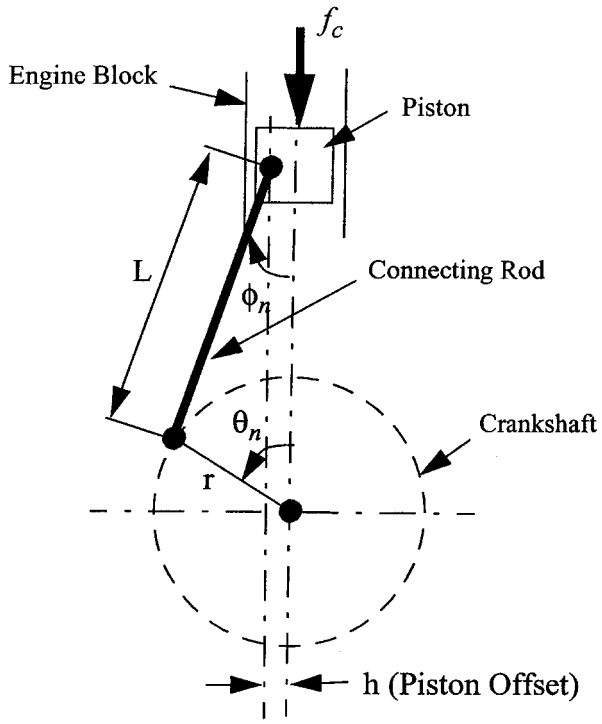

Figure 4. Piston-connecting rod system.

2.4. CONNECTING-ROD OBLIQUE ANGLE IN TERMS OF THE GENERALIZED COORDINATES

Figure 3a shows a block diagram of the example engine structure. Inspection of Figure 3a, reveals six modeling chains that form closed kinematic loops, as shown in Figure 3b. To derive the equations in terms of only the independent coordinates, one needs to cut the modeling chain to form an open loop. Figure 3b shows the modeling chain cut at the link between the piston and the engine block. Next, we will discuss how this can be done without adding additional constraints.

Figure 4 illustrates the structure of the piston-connecting rod system for the nth cylinder, where θ_n is the rotation angle of the center line of the crankshaft throw measured from the center line of the cylinder. Note that θ_n, in general, is a function of the crankshaft angle, the firing angle of the nth cylinder, and the angular deformation due to torsional vibration of the crankshaft at the nth crankshaft throw. ϕ_n stands for the connecting-rod oblique angle of the nth piston-connecting rod system. In the development above, ϕ_n ($n = 1, 2, \ldots, n_{\text{cylinder}}$) are used but they are also dependent on the generalized coordinates as shown next.

Refer to Figure 4 and let L be the length of the connecting rod, r the radius of the crankshaft throw, and h the piston offset. Then,

$$\sin\phi_n = r_L \sin\theta_n - h_L \tag{17}$$

or

$$\phi_n = \text{asin}\,(r_L \sin\theta_n - h_L), \tag{18}$$

where $r_L = r/L$ and $h_L = h/L$. Differentiating Equation (18), once and then again yields

$$\dot{\phi}_n = a_1\dot{\theta}_n \quad \text{and} \quad \ddot{\phi}_n = a_1\ddot{\theta}_n + a_2\dot{\theta}_n^2, \tag{19}$$

where

$$a_1 = \frac{r_L\cos\theta_n}{\cos\phi_n} \quad \text{and} \quad a_2 = \left(\frac{r_L^2\cos^2\theta_n\sin\phi_n}{\cos^3\phi_n} - \frac{r_L\sin\theta_n}{\cos\phi_n}\right).$$

Also we have

$$\delta\phi_n = a_1\delta\theta_n. \tag{20}$$

Equations (18–20) are used to calculate the angle, angular velocity, angular acceleration, and virtual displacement of the connecting-rod oblique angle in term of θ_n, where θ_n is a function of the generalized coordinates. As a result, the constraint equations for the pistons and the cylinders are eliminated by using Equations (18–20).

3. Use of D'Alembert's Principle

D'Alembert's principle (e.g., [26, 27]) is written here in a form that is convenient for automatically deriving the equations of motion of a multi-body system through a symbolic calculation code, e.g., Maple or Matlab. Assume that $\mathbf{q} = \{q_i(t)\}$ (where $i = 1, 2, \ldots, n_{\text{dof}}$) is a set of n_{dof} generalized coordinates, that describes the configuration of the multibody system. Then, let $\dot{\mathbf{q}} = \{\dot{q}_i\}, \ddot{\mathbf{q}} = \{\ddot{q}_i\}$, and $\boldsymbol{\delta}\mathbf{q} = \{\delta q_i\}$ denote the generalized speeds, generalized accelerations, and virtual displacements, respectively. D'Alembert's principle provides the equations of motion from

$$\delta W = 0; \quad \forall\boldsymbol{\delta}\mathbf{q}, \tag{21}$$

where $\delta W = \delta W(\boldsymbol{\delta}\mathbf{q}, \mathbf{q}, \dot{\mathbf{q}}, \ddot{\mathbf{q}})$ denotes the total virtual work done by all forces in the system at time t, including inertia forces, gravity, conservative forces, dissipative forces, and combustion forces, and where $\boldsymbol{\delta}\mathbf{q}$ satisfies all of the kinematic constraints.

We select the generalized coordinates for the engine model so that they are independent. In this case, Equation (21) gives a set of n_{dof} independent ODEs, which can be written in the form

$$(\delta W)_{,\delta q_i} = 0 \quad (i = 1, 2, \ldots, n_{\text{dof}}), \tag{22}$$

where $_{,x} = \partial/\partial x$. Equation (22) can be further rewritten as

$$\mathbf{M}\ddot{\mathbf{q}} = \mathbf{Q}, \tag{23}$$

where $\mathbf{M} = (M_{ij})_{n_{\text{dof}} \times n_{\text{dof}}}$ denotes the generalized mass matrix of the engine system, and $\mathbf{Q} = (Q_j)_{n_{\text{dof}} \times 1}$ denotes the generalized force vector given by

$$M_{ij} = -(\delta W)_{,\delta q_i \ddot{q}_j} \quad (i, j = 1, 2, \ldots, n_{\text{dof}}), \tag{24}$$

$$Q_i = (\delta W)_{,\delta q_i} + \sum_{j=1}^{n_{\text{dof}}} M_{ij}\ddot{q}_j \quad (i = 1, 2, \ldots, n_{\text{dof}}). \tag{25}$$

Note that $Q_i = Q_i(\mathbf{q}, \dot{\mathbf{q}})$ is a function of the generalized coordinates $\mathbf{q}$ and generalized speeds $\dot{\mathbf{q}}$. The terms containing $\ddot{q}_j$ in the left side of Equation (25) will be canceled by the same terms (with the opposite signs) from $(\delta W)_{,\delta q_i}$ (by the symbolic calculation).

Equation (23) can be cast in standard form for first order ODEs and then solved by a standard ODE solver. Equations (24) and (25) can be used to calculate the generalized mass matrix and generalized force vector by a symbolic calculation code such as Maple or Matlab provided the virtual work δW is known as an explicit function of the generalized coordinates $\mathbf{q}$. The critical step in this approach is to derive the explicit form of the virtual work defined in Equation (21), and this will be described in the following section.

4. Virtual Work

The total virtual work of the engine system can be decomposed into the following contributions

$$\begin{aligned}\delta W \;=\; & \delta W_{\text{inertia}} + \delta W_{\text{gravity}} + \delta W_{\text{combustion}} + \delta W_{\text{mount}} \\ & + \delta W_{\text{bearing}} + \delta W_{\text{deformation}} + \delta W_{\text{load}} \,.\end{aligned} \tag{26}$$

Here, $\delta W_{\text{inertia}}$ denotes the virtual work done by all inertia forces in the system including those acting upon the engine block, crankshaft, connecting rods, pistons, balance shafts, counterweights, etc. $\delta W_{\text{gravity}}$ denotes the virtual work done by gravity on these same components, $\delta W_{\text{combustion}}$ denotes the virtual work done by the combustion forces and friction forces on the pistons, δW_{mount} denotes the virtual work done by the elastic and dissipative forces at the engine mounts, $\delta W_{\text{bearing}}$ denotes the virtual work done by the main bearings, $\delta W_{\text{deformation}}$ denotes the virtual work due to flexible crankshaft deformation, and δW_{load} is the virtual work due to all other external loads.

4.1. VIRTUAL WORK OF INERTIA FORCES

The virtual work of the inertia forces are obtained by superposing their contributions from each individual body, i.e.,

$$\delta W_{\text{inertia}} = \sum_{n=1}^{n_{\text{body}}} \delta w_{\text{inertia}}^{(n)}, \tag{27}$$

where the index $n (n = 1, 2, \ldots, n_{\text{body}})$ identifies each body in the engine system, n_{body} denotes the total number of bodies. Here,

$$\delta w_{\text{inertia}}^{(n)} = \int_{\Omega_n} \delta \mathbf{r}_1^{(n)} \cdot (-\rho^{(n)} \ddot{\mathbf{r}}_1^{(n)}) \, \mathrm{d}\Omega, \tag{28}$$

where $\delta \mathbf{r}_1^{(n)}$ denotes the virtual displacement (vector) of a differential element of mass $\rho^{(n)} \, \mathrm{d}\Omega$ in body n, $\ddot{\mathbf{r}}_1^{(n)}$ denotes the acceleration of the same differential element, $\rho^{(n)}$ denotes the mass density of body n, (note that the material density will, in general, vary from body to body) and Ω_n denotes the volume (domain of integration) of body n. Note that both $\delta \mathbf{r}_1^{(n)}$ and $\ddot{\mathbf{r}}_1^{(n)}$ are measured in the global coordinate system $o_1 - x_1 y_1 z_1$. As a result, $\delta \mathbf{r}_1^{(n)}$ is a function of the generalized coordinates, $\mathbf{q}$, and the virtual displacements, $\boldsymbol{\delta}\mathbf{q}$ while $\ddot{\mathbf{q}}_1^{(n)}$ is a function of the generalized coordinates $\mathbf{q}$, velocities $\dot{\mathbf{q}}$ and accelerations $\ddot{\mathbf{q}}$. These functions are constructed using the kinematical relations for the engine as discussed in the previous section.

Only the inertia forces contribute to the generalized mass matrix $\mathbf{M}$ in Equation (23), and therefore substituting Equation (28) into Equation (24), yields

$$M_{ij} = \sum_{n=1}^{n_{\text{body}}} (-\delta w_{\text{inertia}}^{(n)})_{,\delta q_i \ddot{q}_j} \quad (i, j = 1, 2, \ldots, n_{\text{dof}}). \tag{29}$$

Inspection of Equation (29) reveals that the generalized mass matrix can be constructed by simply superposing the contributions from each body in the engine system, i.e.,

$$\mathbf{M} = \sum_{n=1}^{n_{\text{body}}} \mathbf{M}^{(n)}, \tag{30}$$

where $M_{ij}^{(n)} = (-\delta w_{\text{inertia}}^{(n)})_{,\delta q_i \ddot{q}_j} (i, j = 1, 2, \ldots, n_{\text{dof}})$ are related to body n only. This feature provides a natural way to decompose the overall engine system into subsystems and components and to assemble the subsystems' matrices to form the system's matrix.

4.2. VIRTUAL WORK OF GRAVITY

In an analogous manner, the virtual work done by gravity forces is obtained by superposing the virtual work done by gravity on each individual body in the system, i.e.,

$$\delta W_{\text{gravity}} = \sum_{n=1}^{n_{\text{body}}} \delta w_{\text{gravity}}^{(n)}, \tag{31}$$

where

$$\delta w_{\text{gravity}}^{(n)} = \int_{\Omega_0} \delta \mathbf{r}_1^{(n)} \cdot (\rho \mathbf{g})\, \mathrm{d}\Omega, \tag{32}$$

where $\delta \mathbf{r}_1^{(n)}$ denotes the same virtual displacement vector as defined in Equation (28), and $\mathbf{g}$ denotes gravity (vector).

4.3. VIRTUAL WORK OF COMBUSTION FORCES AND FRICTION FORCES

The virtual work of combustion force and friction force acting between the nth piston and the engine block is written as

$$\delta w_{\text{combustion}}^{(n)} = \boldsymbol{\delta} \mathbf{r}_{\text{piston}}^{(n)} \cdot \mathbf{f}_{\text{combustion}}^{(n)}, \tag{33}$$

where $\delta \mathbf{r}_{\text{piston}}^{(n)}$ denotes the relative virtual displacement between the nth piston and the engine block at the point where the combustion force is applied, and $\mathbf{f}_{\text{combustion}}^{(n)}$ denotes the summation of the combustion and friction forces acting between the nth piston and the engine block. Both $\delta \mathbf{r}_{\text{piston}}^{(n)}$ and $\mathbf{r}_{\text{combustion}}^{(n)}$ can be measured in the engine block coordinate system. Note that the friction force represents the resistance caused by the friction between the piston and cylinder wall. It is assumed that the friction force (after lumping) is acting at the some point where the combustion force is applied, though this assumption can be relaxed if the actual distribution of the friction force is known.

Let n_{cylinder} be the number of the cylinders and the virtual work contributed by all piston combustion/friction forces becomes

$$\delta W_{\text{combustion}} = \sum_{n=1}^{n_{\text{cylinder}}} \delta w_{\text{combustion}}^{(n)}. \tag{34}$$

4.4. VIRTUAL WORK OF ENGINE MOUNT FORCES

The engine mounts generate forces as functions of the relative displacement and the relative velocity between the engine block and the vehicle at the mounting point, i.e.,

$$\mathbf{f}_{\text{mount}}^{(n)} = \mathbf{f}_{\text{mount}}^{(n)}\,(\mathbf{r}_{\text{mount}}^{(n)}, \dot{\mathbf{r}}_{\text{mount}}^{(n)}), \tag{35}$$

where $\mathbf{r}_{\text{mount}}^{(n)}$ is the relative displacement at the nth mount, and $\dot{\mathbf{r}}_{\text{mount}}^{(n)}$ is the relative velocity at the same mount. $\mathbf{r}_{\text{mount}}^{(n)}$ and $\dot{\mathbf{r}}_{\text{mount}}^{(n)}$ can be calculated in terms of the generalized coordinates and the velocities of the generalized coordinates, i.e.,

$$\mathbf{r}_{\text{mount}}^{(n)} = \mathbf{d}_b + (\tilde{\mathbf{r}}_2^{\text{mount}(n)})^T \boldsymbol{\Theta}_b \quad \text{and} \quad \dot{\mathbf{r}}_{\text{mount}}^{(n)} = \dot{\mathbf{d}}_b + (\tilde{\mathbf{r}}_2^{\text{mount}(n)})^T \dot{\boldsymbol{\Theta}}_b, \tag{36}$$

where $\mathbf{r}_2^{\text{mount}(n)}$ is the position vector of the nth mount measured in the block coordinate system.

In general, $\mathbf{f}_{\text{mount}}^{(n)}$ is a nonlinear function of the generalized coordinates and it depends on the stiffness and damping characteristics of the engine mount. For the examples in this paper, a linear elastic bushing model is used for the engine mounts for comparison with an ADAMS engine model, that employs the same bushing model. A nonlinear viscoelastic bushing model such as one proposed in [28] could also be employed in the current engine model. Note that the effects of the rotational stiffness and rotational damping of the engine mounts are presently ignored, although they may also be added in a straight-forward manner if known.

The virtual work of the engine mount forces in the nth engine mount is

$$\delta w_{\text{mount}}^{(n)} = \delta \mathbf{r}_{\text{mount}}^{(n)} \cdot \mathbf{f}_{\text{mount}}^{(n)}, \tag{37}$$

where $\delta \mathbf{r}_{\text{mount}}^{(n)} = \delta \mathbf{d}_b + (\tilde{\mathbf{r}}_2^{\text{mount}(n)})^T \delta \boldsymbol{\Theta}_b$ denotes the virtual displacement of the engine block at the location of the nth engine mount relative to the vehicle body. Let n_{mount} be the total number of the engine mounts and the total virtual work done by all engine mounts is

$$\delta W_{\text{mount}} = \sum_{n=1}^{n_{\text{mount}}} \delta w_{\text{mount}}^{(n)}. \tag{38}$$

4.5. VIRTUAL WORK OF MAIN BEARING FORCES

The journal bearings produce forces as functions of the relative displacement and relative velocity between the crankshaft and the engine block at the main journals, i.e.,

$$\mathbf{f}_{\text{bearing}}^{(n)} = \mathbf{f}_{\text{bearing}}^{(n)}\,(\mathbf{r}_{\text{journal}}^{(n)}, \dot{\mathbf{r}}_{\text{journal}}^{(n)}), \tag{39}$$

where $\mathbf{r}_{\text{journal}}^{(n)}$ is the relative displacement at the nth main journal, and $\dot{\mathbf{r}}_{\text{journal}}^{(n)}$ is the relative velocity at the same main journal. $\mathbf{r}_{\text{journal}}^{(n)}$ and $\dot{\mathbf{r}}_{\text{journal}}^{(n)}$ can be calculated in terms of the generalized coordinates and their derivatives, i.e.,

$$\mathbf{r}_{\text{journal}}^{(n)} = \mathbf{d}_c - \mathbf{d}_b + (\tilde{\mathbf{r}}_2^{\text{journal}(n)})^T(\boldsymbol{\Theta}_c - \boldsymbol{\Theta}_b), \tag{40}$$

$$\dot{\mathbf{r}}_{\text{journal}}^{(n)} = \dot{\mathbf{d}}_c - \dot{\mathbf{d}}_b + (\tilde{\mathbf{r}}_2^{\text{journal}(n)})^T(\dot{\boldsymbol{\Theta}}_c - \dot{\boldsymbol{\Theta}}_b), \tag{41}$$

where $\mathbf{r}_2^{\text{journal}(n)}$ is the position vector of the nth main journal measured in the block coordinate system.

The bearing models employed in this paper include: (1) a linear spring-damper model (that is also used by commercial multibody dynamics codes), (2) a nonlinear spring-damper model, and (3) a hydrodynamic model based on the Reynold's equation.

4.5.1. *Linear Spring-Damper Bearing Model*

The linear spring-damper bearing model is defined by a linear force-eccentricity relationship

$$\mathbf{f} = -k\mathbf{e} - c\dot{\mathbf{e}}, \tag{42}$$

where $\mathbf{f}$ denotes the bearing force vector, $\mathbf{e}$ and $\dot{\mathbf{e}}$ denote the vectors of eccentricity and eccentricity rate, and k and c denote the stiffness and damping coefficients of the bearing.

4.5.2. *Nonlinear Spring-Damper Bearing Model*

The nonlinear spring-damper bearing model is defined by the force-eccentricity relationship

$$\mathbf{f} = -k_0 \left(\frac{k_1}{k_0}\right)^{|\frac{e}{e_1}|} \mathbf{e} - c_0 \left(\frac{c_1}{c_0}\right)^{|\frac{e}{e_1}|}, \tag{43}$$

where k_0 and c_0 denote the stiffness and damping of the bearing at $e = |\mathbf{e}| = 0$, k_1 and c_1 denote the stiffness and damping of the bearing at $e = e_1$, and e_1 is a given reference value of the eccentricity.

4.5.3. *Hydrodynamic Bearing Models*

The hydrodynamic bearing models employed herein are based on the special solutions of the Reynold's equation (refer to [29, 30]). For example, in the so-called 'short bearing' case, we have

$$f_x = \frac{\mu R L^3 V_s}{C^3} \int_{\theta_1}^{\theta_2} \frac{1}{h^3} \cos(\theta + \alpha) \cos(\theta + \beta)\, \mathrm{d}\theta, \tag{44}$$

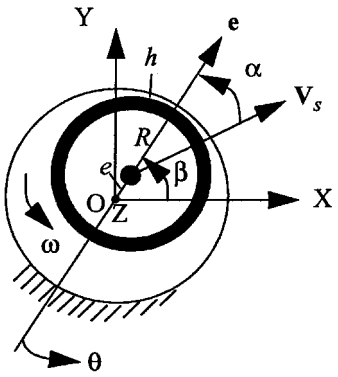

Figure 5. Variables of a main journal bearing.

$$f_y = \frac{\mu R L^3 V_s}{C^3} \int_{\theta_1}^{\theta_2} \frac{1}{h^3} \cos(\theta + \alpha) \sin(\theta + \beta)\, \mathrm{d}\theta, \tag{45}$$

where $\mathbf{f} = \{f_x, f_y\}^T$, μ denotes the fluid viscosity, R denotes the journal radius, L denotes the length of the journal, C denotes the journal clearance, V_s is termed the journal's 'pure-squeeze-velocity', α is the angle between the journal's pure-squeeze-velocity vector and the eccentricity vector (Figure 5), h is the normalized film thickness defined by

$$h = 1 + \varepsilon \cos\theta, \tag{46}$$

where ε is the eccentricity ratio of the journal measured in the polar-cylindrical coordinate system, $\varepsilon = e/C$, θ denotes the angle of the polar-cylindrical coordinates as shown in Figure 5, and β is the angle between the eccentricity vector and the X axis of $O - XY$ as shown in Figure 5.

Note that the integration domain of Equations (44) and (45) can lead to either a π or 2π model for the short bearing. For the short-π bearing model, the limits of integration are $\theta_1 = \pi/2 - \alpha$ and $\theta_2 = 3\pi/2 - \alpha$, and for the short-$2\pi$ bearing model, these limits become $\theta_1 = 0$ and $\theta_2 = 2\pi$.

The virtual work done by the forces in the nth main journal bearing is

$$\delta w^{(n)}_{\text{bearing}} = \delta \mathbf{r}^{(n)}_{\text{journal}} \cdot \mathbf{f}^{(n)}_{\text{bearing}}, \tag{47}$$

where $\delta \mathbf{r}^{(n)}_{\text{journal}} = \delta \mathbf{d}_c - \delta \mathbf{d}_b + (\tilde{\mathbf{r}}_2^{\text{journal}(n)})^T (\delta \boldsymbol{\Theta}_c - \delta \boldsymbol{\Theta}_b)$ denotes the relative virtual displacement between the crankshaft and the engine block at the location of this bearing. Let n_{journal} be the total number of main journals, and therefore the virtual work done by all bearing forces becomes

$$\delta W_{\text{bearing}} = \sum_{n=1}^{n_{\text{journal}}} \delta w^{(n)}_{\text{bearing}}. \tag{48}$$

In the next section, we will give an example that compares results obtained using these three different bearing models, i.e., linear spring-damper, nonlinear spring-damper, and hydrodynamic (typically, short-π).

4.6. VIRTUAL WORK ASSOCIATE WITH FLEXIBLE CRANKSHAFT DEFORMATION

The crankshaft is considered as a flexible body, that may deform during engine operation. Crankshaft vibration is known to influence engine dynamics, a fact reported in many studies; see, for example, [17, 18, 25]. To this end, we employ a modal representation for crankshaft flexibility as shown in Equation (3). From Equation (3) and Equations (6–8) we have

$$\mathbf{r}_1^{(\mathrm{cs})} = \mathbf{r}_1^{(\mathrm{cs-rigid})} + \mathbf{A}_{1,4} \sum_{i=1}^{n_{\mathrm{modes}}} \phi_i \, p_i, \tag{49}$$

where $\mathbf{r}_1^{\mathrm{cs})}$ denotes the position vector of a point on the crankshaft after the crankshaft deformation, $\mathbf{r}_1^{(\mathrm{cs-rigid})}$ denotes the position vector of the same point before crankshaft deformation and $\mathbf{A}_{1,4} = \mathbf{A}_{1,2}\ \mathbf{A}_{2,3}\ \mathbf{A}_{3,4}$. Both $\mathbf{r}_1^{(\mathrm{cs})}$ and $\mathbf{r}_1^{(\mathrm{cs-rigid})}$ are measured in the global coordinate system $o_1 - x_1 y_1 z_1$. Here,

$$\mathbf{r}_1^{(\mathrm{cs-rigid})} = \mathbf{DC}_{1,4}\, \mathbf{R}. \tag{50}$$

By taking the variation of Equation (49), the virtual displacement of any point on the crankshaft can be obtained as

$$\delta\mathbf{r}_1^{(\mathrm{cs})} = \delta\mathbf{r}_1^{(\mathrm{cs-rigid})} + \sum_{i=1}^{n_{\mathrm{modes}}} (\delta\mathbf{A}_{1,4}\, \phi_i \, p_i + \mathbf{A}_{1,4}\, \phi_i \delta p_i). \tag{51}$$

By differentiating Equation (49) twice, we obtain the acceleration of the same point on the crankshaft

$$\ddot{\mathbf{r}}_1^{(\mathrm{cs})} = \ddot{\mathbf{r}}_1^{(\mathrm{cs-rigid})} + \sum_{i=1}^{\mathrm{n_{modes}}} (\ddot{\mathbf{A}}_{1,4}\, \phi_i \, p_i + 2\dot{\mathbf{A}}_{1,4}\, \phi_i \, \dot{p}_i + \mathbf{A}_{1,4}\, \phi_i \, \ddot{p}_i), \tag{52}$$

where $\dot{p}_i$, $\ddot{p}_i$, δp_i denote the velocity, acceleration, and virtual displacement associated with p_i.

Equations (51) and (52) are substituted into Equation (28) (where $n = \mathrm{cs}$) to calculate the virtual work of the crankshaft inertia forces. As shown in Equation (49), if $n_{\mathrm{modes}} = 0$, $\mathbf{r}_4^{(\mathrm{cs})} = \mathbf{r}_4^{(\mathrm{cs-rigid})}$, and the crankshaft model reduces to that of a rigid body. On the other hand, crankshaft models of increasing fidelity can be constructed by adding selected higher order crankshaft modes in sequence.

The virtual work done by the internal stresses of the crankshaft can be written as

$$\delta w_{\text{deformation}} = -\int_{\Omega_{\text{cs}}} \boldsymbol{\delta\varepsilon} \bullet \boldsymbol{\sigma}\, \mathrm{d}\Omega, \tag{53}$$

where $\boldsymbol{\delta\varepsilon}$ denotes the strain tensor due to the virtual deformation, $\boldsymbol{\sigma}$ is the stress tensor due to the same virtual deformation, and $\bullet$ denotes a tensor product. The domain of integration in Equation (53) is the domain (volume) of the crankshaft Ω_{cs}. If modal coordinates are used as the generalized coordinates, then this virtual work can be recast as

$$\delta w_{\text{deformation}} = -\sum_{i=1}^{\text{n}_{\text{modes}}} \delta p_i(\omega_i^2 p_i + 2\xi_i \omega_i \dot{p}_i), \tag{54}$$

where ω_i are the natural frequencies of the crankshaft, and ξ_i denotes the companion modal damping ratios. Note that the virtual work contributed by dissipation within the crankshaft is captured in Equation (54) by the use of modal damping.

The mode shapes above are defined by prescribing the relative displacement at selected points along the crankshaft. For instance, the relative displacements at the main bearings, at the connecting rod bearing points, and/or at the locations of the counterweights are required. Thus, it is not necessary to have a full (functional) representation of the crankshaft mode shapes, only a discretized representation at these selected points. This feature makes this model attractive for upfront engine design since a detailed design of the crankshaft may not be available.

Finally, note that the crankshaft vibration modes, natural frequencies and damping ratios can also be obtained from analytical crankshaft models, finite element models, experimental measurements, or estimates based on similar designs. The modal parameters could also be prescribed as requirements for crankshaft design in support of target cascading.

5. Example Results

The primary purpose of this paper is to summarize the formulation of a general engine model. Preliminary results will now be described pertaining to an example engine already in production. The first results describe the free (idealized) motion of this engine system. This is followed by results that describe forced motion due to engine combustion forces.

5.1. FREE MOTION

In the first example, eleven rigid body modes of a Ford V-6 engine are predicted using the engine model developed in this paper. Figure 6 illustrates how the natural frequencies of these eleven modes vary with the rotation (position) of the crankshaft. Here, the first six modes govern the free vibration of the engine block which

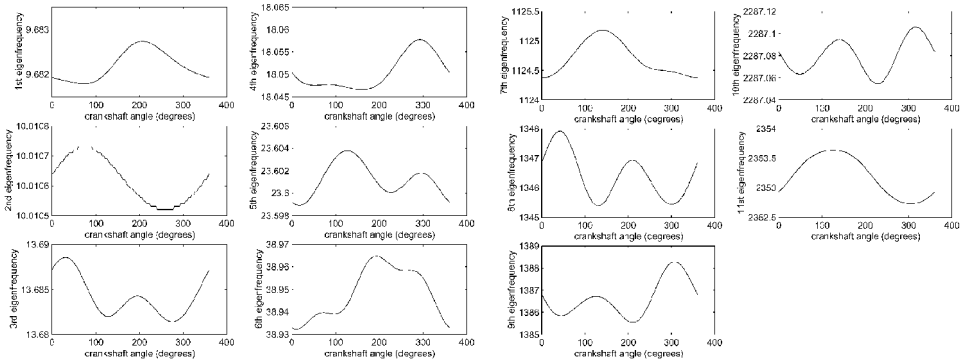

Figure 6. Natural frequencies of engine modes vs. crankshaft angle.

rests on four engine mounts. The last five modes govern the free vibration of the (rigid) crankshaft which is captured by the four main bearings. Both the engine mount and bearing models are linearized for the purpose of this calculation. As shown in Figure 6, the rotation of the crankshaft influences the motion of the pistons, connecting rods and other engine components and hence alters the system mass distribution to a modest degree as reflected in the results of Figure 6. Note that at most, this effect produces a 2 Hz change in the natural frequencies of the eighth and ninth modes which correspond to the lateral and yaw vibrations of the crankshaft, respectively.

5.2. FORCED MOTION

We now consider three different cases of forced response. In the two of these cases, the crankshaft is driven at a constant speed of 600 rpm. In the first case, the main bearings are considered rigid, and in the second case, the main bearings are represented by a linear springdamper model. Both results are obtained using the engine model developed in this paper, and also compared to an equivalent model constructed using ADAMS. The third case extends the calculation to include different bearing models. To this end, we will compare three different bearing models, including the linear, nonlinear, and hydrodynamic (short-π) bearing models described herein.

Figure 7 provides a comparison of the predicted mount forces on the rear-right engine mount with the results obtained from an ADAMS simulation for the first case (rigid bearings). The three force components, F_x, F_y and F_z in Figure 7, describe respectively the mount force components along the global x, y, and z directions at the rear-right engine mount. As shown in Figure 7, the engine mount responds nearly harmonically at the frequency of crankshaft rotation, and both models predict almost the same results (aside from a different starting transient). (The differences in the starting transient derive from the fact that the ADAMS

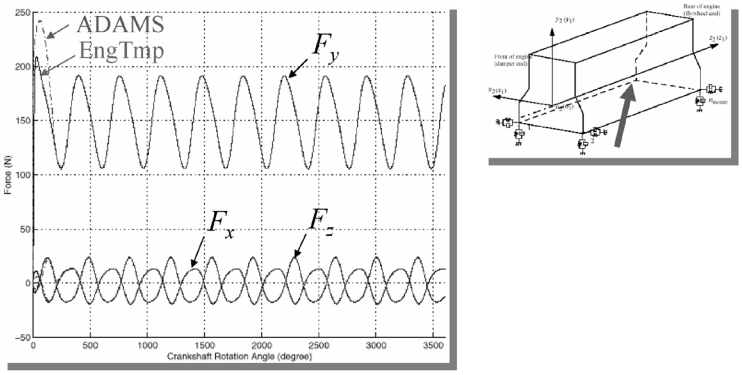

Figure 7. Comparison of mount forces predicted by the engine model template (*EngTmp*) with results obtained using an ADAMS model for the case of rigid bearings.

model cannot start instantaneously from a non-zero value of crankshaft rotation speed.)

Note that in the ADAMS model, there are 15 rigid bodies possessing 90 generalized coordinates to describe the configuration of the example engine. Since there are only 6 independent coordinates in this engine model (the rigid body coordinates of the engine block), the ADAMS model requires 84 kinematic constraints in the form of algebraic equations. The new formulation developed in this paper employs only six independent generalized coordinates in the form of ODEs, which in general can be integrated more efficiently and with greater numerical stability.

Also note that in the engine model developed in this paper, the second and higher order terms in terms of the engine block rotations have been ignored in the engine kinematics. Those terms however are not ignored in the ADAMS model. As shown by the Figure 7, the loss of these higher order terms has no appreciable effect on accuracy in this example.

Consider now results obtained using the linear spring-damper bearing model. Figure 8 shows a comparison with results obtained by ADAMS for the amplitude of the predicted bearing force in the first main bearing. In this figure, the solid line represents results obtained by the engine template while the dashed line shows the results obtained by ADAMS. These results are in very close agreement with maximum difference in the peak values of less than 2%. This small difference derives mainly from the fact that the ADAMS model can not drive the crankshaft at the constant speed about the crankshaft axis (i.e., z_3 axis of $o_3 - x_3 y_3 z_3$), but only at the constant speed about the longitudinal axis of the global coordinate system (i.e., z_1 axis of $o_1 - x_1 y_1 z_1$). This difference generates slightly different driving torques on the crankshaft, and leads to the small differences shown in Figure 7.

The last case of this example provides a comparison of the bearing force component, F_x (i.e., lateral bearing force in the engine block coordinate system), as predicted by three different bearing models, namely, the linear spring-damper bearing model, the nonlinear spring-damper bearing model, and the hydrodynamic

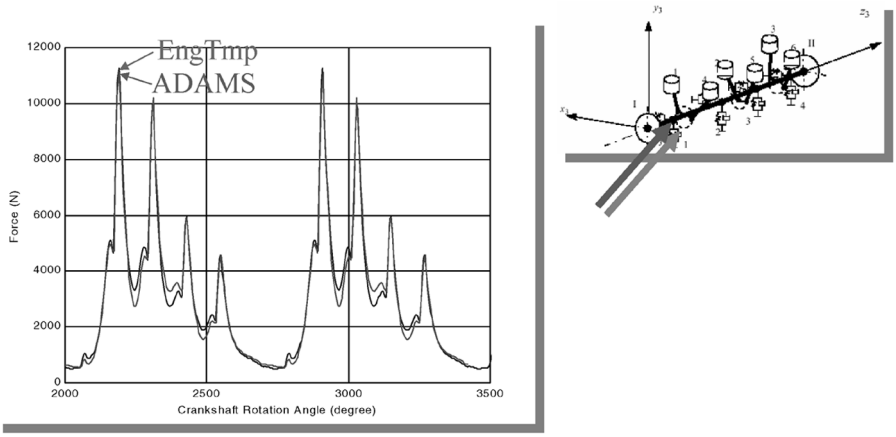

Figure 8. Comparison of bearing force predicted by the engine model template (*EngTmp*) with results obtained using an ADAMS model for the case of the linear spring-damper bearing model.

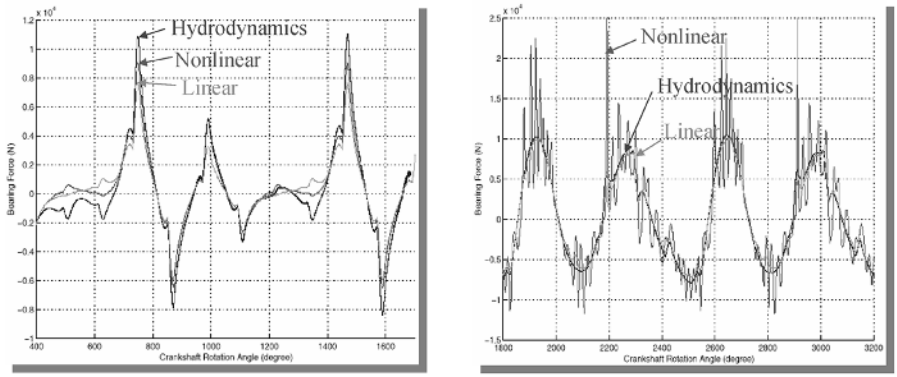

(a) 600 rpm (b) 6,000 rpm

Figure 9. Comparisons of bearing force for different bearing models.

bearing model (short-π model, see Equations (44–46)). Figure 9a illustrates this comparison for the crankshaft is driven at 600 rpm, while Figure 9b shows results for the crankshaft is driven at 6,000 rpm. As shown in Figure 9a, the maximum difference in predicted peak bearing force between the linear and the hydrodynamic models is about 17%, while the difference between the nonlinear and the hydrodynamic models is less than 2%. Therefore, in this case, the nonlinear model more closely predicts the bearing forces predicted by the hydrodynamic bearing model. However, this conclusion is reversed when evaluating the results for the higher crankshaft speed. Figure 9b shows that, at this higher crankshaft rotation speed, the nonlinear bearing model predicts a large amplitude, high-frequency oscillation in

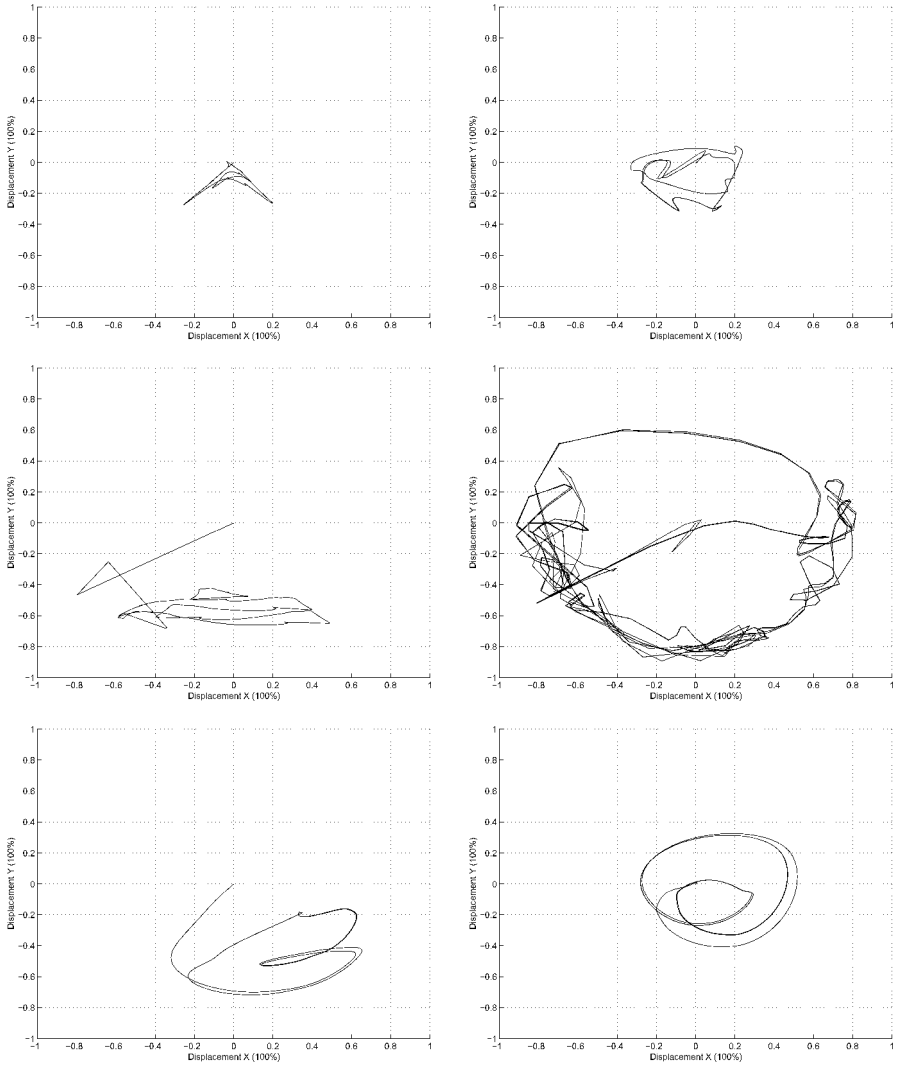

Figure 10. Orbit plots of crankshaft: (a–c) crankshaft is driven at 600 rpm, (d–f) crankshaft is driven at 6,000 rpm; (a) and (d) linear spring-damper bearing model, (b) and (e) nonlinear spring-damper model, (c) and (f) hydrodynamic bearing model (short-π).

the bearing force that is not apparent in either the linear and hydrodynamic bearing models which are also in close agreement.

Figure 10 provides a further comparison of these three results by illustrating the orbits of the journal center for the cases discussed above. Figures 10a–10c show the orbits for the case of 600 rpm, while Figure 10d–10f correspond to the case of 6,000 rpm. Figure 10a and 10d show the results obtained by using the linear bearing model, Figure 10b and 10e the results obtained by using the nonlinear bearing model, and Figures 10c and 10f the results obtained by using the

hydrodynamic bearing model. As shown in Figure 10, the use of different bearing model predict very different behaviors of these orbits despite the relatively good agreement achieved for the predicted bearing forces. Also, Figure 10 shows that the linear and nonlinear bearing models predict very different behaviors at the two different speeds of the crankshaft rotation, while the hydrodynamic bearing model predicts qualitatively similar behavior. Finally, note that comparisons for different hydrodynamic bearing models can be found in [30].

6. Summary

This paper summarizes an engine model that can be used to support 'up-front' (i.e., early) engine design. This engine model captures the dynamic response of an engine at frequencies commensurate with the rigid body modes of the engine and crankshaft, as well as the low order vibration modes of the crankshaft. A recursive formulation is proposed to formulate the engine multi-body dynamics model. The use of the relative coordinates as the generalized coordinates results in a minimal set of ordinary differential equations governing engine dynamics. D'Alembert's principle is used to derive the equations of motion. These equations are expressed in terms of a generalized mass matrix and generalized force vector by using a symbolic calculation code, such as Maple or Matlab, and then reduced automatically to computational code (C or Fortran) for numerical integration. The engine model follows from the kinematical relations needed to represent the engine dynamics in terms of the selected generalized coordinates and the systematic analysis of the virtual work done by all forces acting in the engine system. Initial results obtained from this engine model are presented for a production engine including both free and forced engine motion.

These results of this paper represent the first step towards the future development of an *engine modeling template* to support up-front engine design. The *EngTmp* will take the form of menu-driven software that will allow an engine designer to automatically build a model for engine dynamics from relatively general design information. The menu will also permit the designer to automatically evaluate engine noise and vibration targets. By automating this process, the engine designer will be free to explore widely differing design concepts at the start of the design cycle and to check critical engine performance metrics in an efficient manner.

Appendix: Definitions of Coordinate Systems

Seven coordinate systems, $o_i - x_i y_i z_i$ ($i = 1, 2, \ldots, 7$), are defined in Figures 11 to 18 for the engine model, where $o_1 - x_1 y_1 z_1$ (Figure 11) is called vehicle coordinate system and is fixed at the vehicle body and assumes the role of the global coordinate system. $0_2 - x_2 y_2 z_2$ (Figure 11) is called the block coordinate system and is fixed at the engine block. $0_3 - x_3 y_3 z_3$ (Figure 12) is called the crankshaft floating coordinate

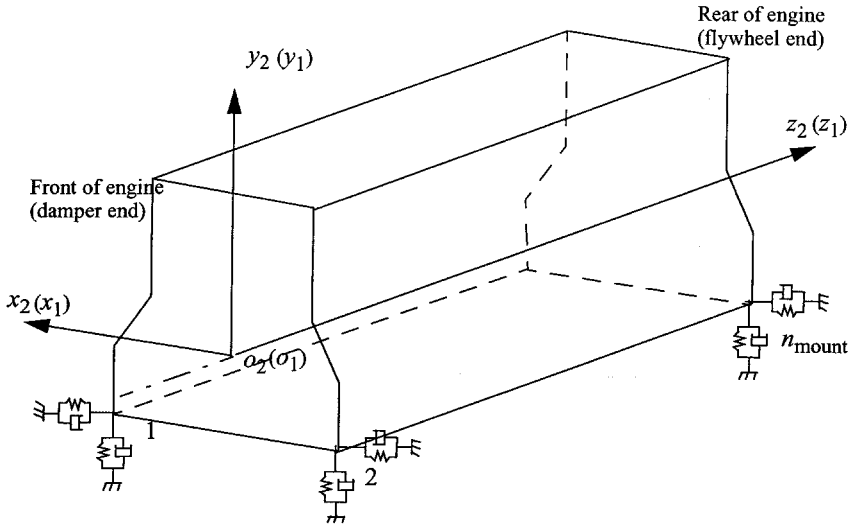

Figure 11. Block coordinate system.

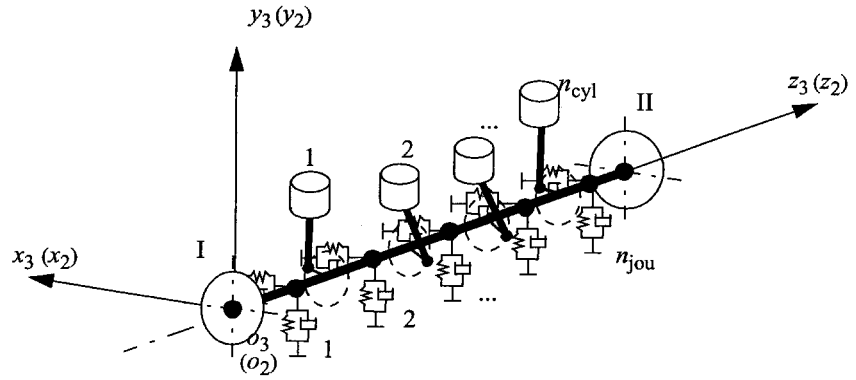

Figure 12. Crankshaft floating coordinate system.

system and is attached to the axis of the crankshaft, but not rotating about this axis with the crankshaft. Note that the coordinate systems of $o_i - x_i y_i z_i (i = 1, 2, 3)$ initially have the same origins at the first main bearing of the crankshaft, and the same orientation as shown in Figures 11 and 12. $o_4 - x_4 y_4 z_4$ (Figure 13) is called the crankshaft fixed coordinate system and is fixed on the crankshaft and rotates fully with it. As shown in Figure 13, $o_4 - x_4 y_4 z_4$ has the same origin as $o_3 - x_3 y_3 z_3$, but is initially rotated by -β about the z_3 axis of $o_3 - x_3 y_3 z_3$, where β denotes the half bank angle as illustrated in Figure 13. Thus, the y_4 axis of $o_4 - x_4 y_4 z_4$ is parallel to the axis of the first cylinder. $o_5 - x_5 y_5 z_5$ (Figure 14) is called the crankshaft throw coordinate system and is attached to a crankshaft throw as shown in Figure 14. Since there are a total number of n_{cyilnder} crankshaft throws, an additional superscript n is used to identify that the coordinate system is associated with

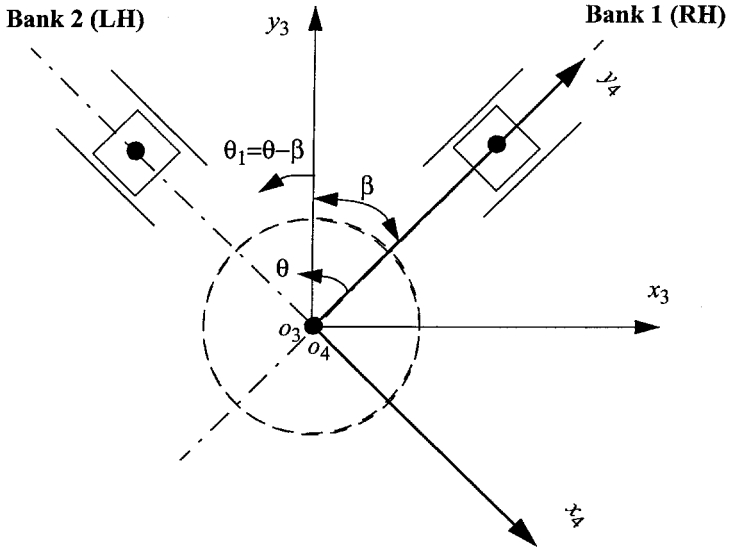

Figure 13. Crankshaft fixed coordinate system.

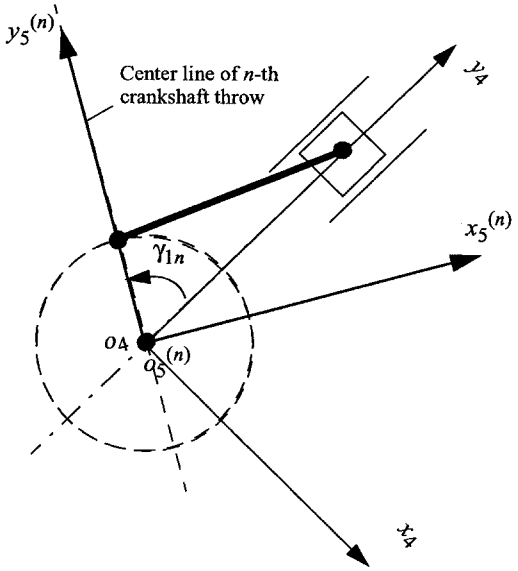

Figure 14. Crankshaft throw coordinate system.

the nth crankshaft throw. $o_6 - x_6y_6z_6$ (Figures 15 and 16) is called the connecting-rod coordinate system and is fixed to a connecting rod. The additional superscript n indicates that the coordinate system is associated with the nth connecting rod. Figure 15 shows the connecting rod coordinate system that belongs to the first bank of the engine; Figure 16 shows the connecting rod coordinate system that belongs to the second bank of the engine. Finally, $o_7 - x_7y_7z_7$ (Figures 17 and 18) is called

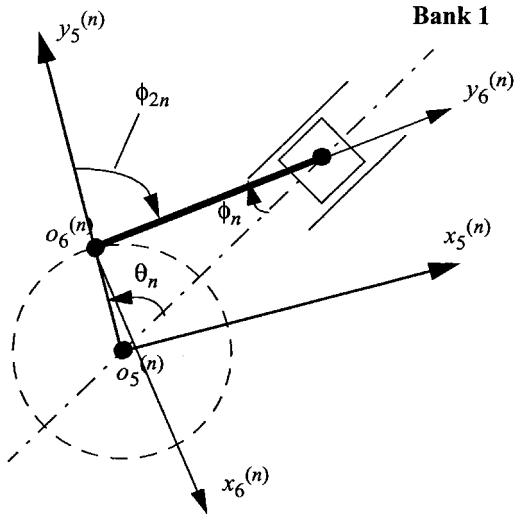

Figure 15. Connecting rod coordinate system (for ninBank1.

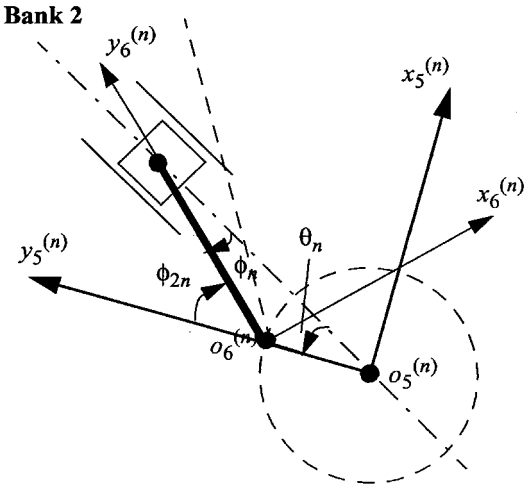

Figure 16. Connecting rod coordinate system (for ninBank2.

the piston coordinate system and is fixed to a piston. The additional superscript n indicates that the coordinate system is associated with the nth piston. Figure 17 shows the piston coordinate system that belongs to BANK 1; Figure 18 shows the piston coordinate system that belongs to BANK 2. Note that for an I-type engine, the bank angle is zero, and all the definitions remain unaltered. For a V-type engine BANK 1 and BANK 2 refer to the piston groups on the right-hand side and the left-hand side of the engine as shown in Figure 13.

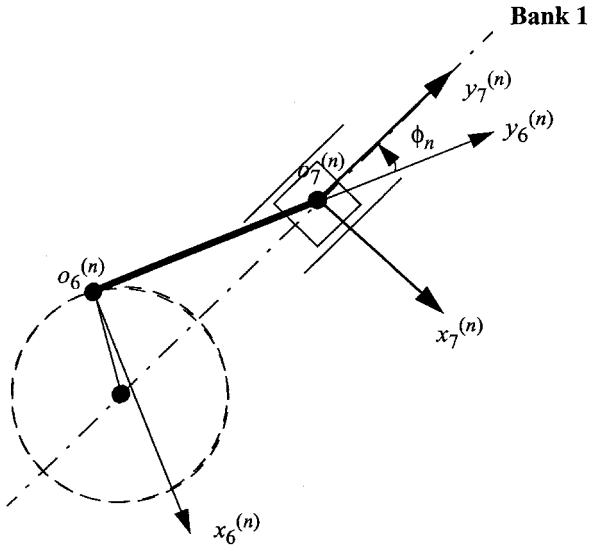

Figure 17. Piston n coordinate system (for $n \in$ Bank1.

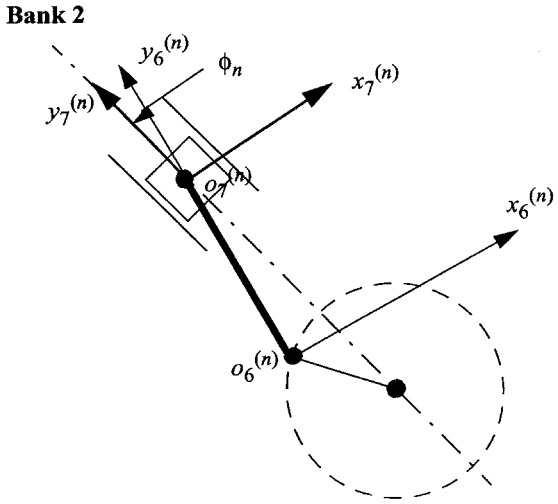

Figure 18. Piston n coordinate system (for $n \in$ Bank2.

Let the notation $i \to i-1$ denote the transformation from coordinate system i to coordinate system $i-1$. Then, for Equation (2) we have:

$$2 \to 1: \quad \mathbf{d}_1 = \begin{Bmatrix} u_b \\ v_b \\ w_b \end{Bmatrix}, \quad \mathbf{A}_{1,2} = \begin{bmatrix} 1 & -\gamma_b & \beta_b \\ \gamma_b & 1 & -\alpha_b \\ -\beta_b & \alpha_b & 1 \end{bmatrix},$$

$$3 \to 2: \quad \mathbf{d}_2 = \begin{Bmatrix} u_c - u_b \\ v_c - v_b \\ w_c - w_b \end{Bmatrix},$$

$$\mathbf{A}_{2,3} = \begin{bmatrix} 1 & -(\gamma_c - \gamma_b) & (\beta_c - \beta_b) \\ (\gamma_c - \gamma_b) & 1 & -(\alpha_c - \alpha_b) \\ -(\beta_c - \beta_b) & (\alpha_c - \alpha_b) & 1 \end{bmatrix},$$

$$4 \to 3: \quad \mathbf{d}_3 = 0, \quad \mathbf{A}_{3,4} = \mathbf{A}(\theta_1),$$

$$5 \to 4: \quad \mathbf{d}_4^{(n)} = \begin{Bmatrix} 0 \\ 0 \\ l_n \end{Bmatrix}, \quad \mathbf{A}_{4,5}^{(n)} = \mathbf{A}(\gamma_{1n}),$$

$$6 \to 5: \quad \mathbf{d}_5^{(n)} = \begin{Bmatrix} 0 \\ r_n \\ 0 \end{Bmatrix}, \quad \mathbf{A}_{5,6}^{(n)} = \mathbf{A}(\phi_{2n}),$$

$$7 \to 6: \quad \mathbf{d}_6 = \begin{Bmatrix} 0 \\ L \\ 0 \end{Bmatrix}, \quad \mathbf{A}_{6,7}^{(n)} = \mathbf{A}(\phi_n),$$

where u_b, v_b, w_b, α_b, β_b, γ_b denote the displacements (angles) of the engine block measured in the vehicle coordinate system, u_c, v_c, w_c, α_c, β_c, γ_c ($\gamma_c \equiv \gamma_b$) denote the displacements (angles) of the crankshaft axis measured in the vehicle coordinate system, I_n denotes the z coordinate of the nth crankshaft throw in the crankshaft coordinate system, r_n denotes the distance between the center of the nth pin journal and the z-axis of the crankshaft coordinate system, L is the length of the connecting rod, and

$$\theta_1 = \theta - \beta,$$

$$\gamma_{1n} = \gamma_n - \varphi_n,$$

$$r_n = r + \varepsilon_n,$$

$$\phi_{2n} = -(\phi_n + \theta_n),$$

$$\theta_n = \theta + \gamma_n - \varphi_n,$$

where β denotes the half bank angle, ϖ_n denotes the firing angle of the nth cylinder, γ_n denotes the torsional deformation angle of the crankshaft at the nth crankshaft throw (which is a function of modal coordinates), r denotes the radius of the crankshaft, ε_n denotes the radial displacement of the center of the nth pin journal measured at the crankshaft-fixed coordinate system (which is also a function of the

modal coordinates), and ϕ_n denotes the oblique angle of the nth connecting rod (which is a function of generalized coordinates as shown in Equation (18)). We also introduce the following definition:

$$\mathbf{A}(\theta) = \begin{bmatrix} \cos\theta & -\sin\theta & 0 \\ \sin\theta & \cos\theta & 0 \\ 0 & 0 & 1 \end{bmatrix} \quad \text{for any angle } \theta.$$

Acknowledgments

The authors would like to acknowledge the original support provided by the Ford Motor Company's Analytical Powertrain Department. The authors also acknowledge the support provided by the U.S. Army Tank-Automotive Command (TACOM) through the University of Michigan Automotive Research Center, a U.S. Army Center of Excellence for Automotive Research, under contract number DAAE07-98-3-0022.

References

1. Hayes, P.A. and Quantz, C.A., 'Determining vibration, radiation efficiency and noise characteristics of structural design using analytical techniques', SAE 820440, 1982.
2. Nefske, D.J. and Sung, S.H., 'Coupled vibration response of the engine crank-block system', in *ASME 12th Biennial Conference on Mechanical Vibration and Noise*, Montreal, Quebec, Canada, ASME, New York, DE-Vol. 18-4, 1989, 379–385.
3. Sohn, K., Honda, S., Okuma, M., Ishii, T. and Nagamatsu, A., 'Basic research on the vibration and noise of internal combustion engines', *JSME International Journal, Series C* **36**(4), 1993, 413–420.
4. Sung, S.H., Nefske, D.J., Chen, F.H.K. and Fannin, M.P., 'Development of an engine system model for predicting structural vibration and radiated noise of the running engine', SAE 972039, 1997.
5. Richardson, S.H. and Riding, D.H., 'Predictive design support in the achievement of refined power for the Jaguar XK8', SAE 972041, 1997.
6. Takahashi, Y., Toshibumi, S. and Tsukahara, M., 'Prediction of powerplant vibration using FRF data of FE model', SAE paper No. 971959, 1997.
7. Loibnegger, B., Rainer, G., Bernard, L., Micelli, D. and Turino, G., 'An integrated numerical tool for engine noise and vibration simulation', SAE 971992, 1997.
8. Sumi, K., Yamamoto, K., and Gielen, L., 'Development of hybrid model for powerplant vibration', SAE 1999-01-1656, 1999.
9. Gomes, E., Breida, M., Kley, P. and Ratliff, M., 'NVH optimization of the 1.2L DIATA Engine', SAE 1999-01-1744, 1999.
10. Radcliffe, C.J., Picklemann, M.N., Hine, D.S. and Spiekermann, C.E., 'Simulation of engine idle shake vibration', SAE 830259, 1983.
11. Bernard, J.E. and Starkey, J.M., 'Engine mount optimization', SAE 830257, 1983.
12. Johnson, S.R. and Subhedar, J.W., 'Computer optimization of engine mounting systems', SAE 790974, 1997.
13. Bretl, J., 'Advancements in computer simulation method for vehicle noise and vibration', SAE 951255, 1995.

14. Snyman, J.A., Heyns, P.S. and Vermeulen, P.J., 'Vibration isolation of a mounted engine through optimization', *Mechanism & Machine Theory* **30**, 1995, 109–118.
15. Muller, M., Siebler, T.W. and Gartner, H., 'Simulation of vibrating vehicle structures as part of the design process of engine mount systems and vibration absorbers', SAE 952211, 1995.
16. Suh, C.-H. and Smith, C.G., 'Dynamic simulation of engine-mount systems', SAE 971940, 1997.
17. Kubozuka, T., Hayashi, Y., Hayakawa, Y. and Kikuchi, K., 'Analytical study on engine noise caused by vibration of the cylinder block and crankshaft', SAE 830346, 1983.
18. Morita, T. and Okamura, H., 'Simple modeling and analysis for crankshaft three-dimensional vibrations, Part 2: Application to an operating engine crankshaft', *ASME Journal of Vibration and Acoustics* **117**(1), 1995, 80–86.
19. Okamura, H., Naganuma, T. and Morita, T., 'Influences of torsional damper temperature and vibration amplitude on the three-dimensional vibrations of the crankshaft-cylinder block system under firing conditions', SAE 1999-01-1775, 1999.
20. Hoffinan, D.M.W. and Dowling, D.R., 'Modeling fully-coupled rigid engine dynamics and vibrations', SAE 1999-01-1749, 1999.
21. Stout, J.L., 'Concept level powertrain radiated noise analysis', SAE 1999-01-1746, 1999.
22. Mayer, L., Zeischka, J. Scherens, M. and Maessen, F., 'Analysis of flexible rotating crankshaft with flexible engine block using MSC/NASTRAN and DADS', in *Proceedings of 1995 MSC World User's Conference*, University City, CA, May 1995, 1–15.
23. Zeischka, J., Kading, D. and Crosheck, J., 'Simulation of flexible engine block, crank, and valvetrain effects using DADS', in *Proceedings of the 1998 Global Powertrain Congress*, Detroit, MI, October, D. Roessler (ed.), 1998, 5–11.
24. Bamford, M., Lin, Y., Jiang, Y. and Harris, B., '3D piston secondary motion', in *Proceedings of the 1998 International ADAMS User Conference*, Mechanical Dynamics, 1998, 1–13.
25. Du, H.Y.I., 'Simulation of flexible rotating crankshaft with flexible engine block and hydrodynamic bearings for a V6 engine', SAE 1999-01-1752, 1999.
26. Haug, E.J., *Computer-Aided Kinematics and Dynamics of Mechanical Systems, Volume I: Basic Methods*, Allyn and Bacon, Boston, MA, 1989.
27. Shabana, A.A., *Dynamics of Multibody Systems*, John Wiley, New York, 1989.
28. Ledesma, R., Ma, Z.-D., Hulbert, G.M. and Wineman, A., 'A nonlinear viscoelastic bushing element in multibody dynamics', *Computational Mechanics* **17**, 1996, 1–10.
29. Ma, Z.-D. and Perkins, N.C., 'A first principle engine model for up-front design', in *Proceedings of the ASME Dynamic Systems and Control Division – 2000*, Orlando, FL, ASME, New York, Volume 1, 2000, 569–576.
30. Ma, Z.-D. and Perkins, N.C., 'A first principle engine model for up-front design: Bearing models and example results', in *Proceedings of a Symposium on Advanced Automotive Technologies*, November 11–16, ASME, New York, 2001, 1–8.